

# Journal Pre-proof

Red light delays programmed cell death in non-host interaction between *Pseudomonas syringae* pv *tomato* DC3000 and tobacco plants

Laura Moyano, María P. Lopéz-Fernández, Analía Carrau, Julián M. Nannini, Silvana Petrocelli, Elena G. Orellano, Sara Maldonado



PII: S0168-9452(19)31534-1  
DOI: <https://doi.org/10.1016/j.plantsci.2019.110361>  
Reference: PSL 110361  
To appear in: *Plant Science*  
Received Date: 10 May 2019  
Revised Date: 22 November 2019  
Accepted Date: 25 November 2019

Please cite this article as: Moyano L, Lopéz-Fernández MP, Carrau A, Nannini JM, Petrocelli S, Orellano EG, Maldonado S, Red light delays programmed cell death in non-host interaction between *Pseudomonas syringae* pv *tomato* DC3000 and tobacco plants, *Plant Science* (2019), doi: <https://doi.org/10.1016/j.plantsci.2019.110361>

This is a PDF file of an article that has undergone enhancements after acceptance, such as the addition of a cover page and metadata, and formatting for readability, but it is not yet the definitive version of record. This version will undergo additional copyediting, typesetting and review before it is published in its final form, but we are providing this version to give early visibility of the article. Please note that, during the production process, errors may be discovered which could affect the content, and all legal disclaimers that apply to the journal pertain.

© 2019 Published by Elsevier.

**Red light delays programmed cell death in non-host interaction between *Pseudomonas syringae* pv *tomato* DC3000 and tobacco plants**

Laura Moyano<sup>1,2†</sup>, María P. López-Fernández<sup>1,2†</sup>, Analía Carrau<sup>3</sup>, Julián M. Nannini<sup>3</sup>, Silvana Petrocelli<sup>4</sup>, Elena G. Orellano<sup>3,4</sup>, Sara Maldonado<sup>1,2</sup>

<sup>1</sup>Departamento de Biodiversidad y Biología Experimental, Facultad de Ciencias Exactas y Naturales, Universidad de Buenos Aires, Buenos Aires, Argentina, <sup>2</sup>Consejo Nacional de Investigaciones Científicas Técnicas, Instituto de Biodiversidad y Biología Experimental y Aplicada, Buenos Aires, Argentina, <sup>3</sup>Consejo Nacional de Investigaciones Científicas y Técnicas, Instituto de Biología Molecular y Celular de Rosario, Rosario, Argentina, <sup>4</sup>Facultad de Ciencias Bioquímicas y Farmacéuticas, Universidad Nacional de Rosario, Rosario, Argentina.

†These authors have contributed equally to this work.

*Corresponding autor:* Maria Paula López -Fernández. Facultad de Ciencias Exactas y Naturales, Universidad de Buenos Aires, Intendente Güiraldes 2160 (C1428EGA) Ciudad de Buenos Aires, Argentina. Tel.: +541145763300; fax: +541145763384.

E-mail addresses: mpaula@bg.fcen.uba.ar, mapaula.lf@gmail.com

### Highlights

- Light modulates the HR of tobacco plants to Pto DC3000 infection
- Red light delays the HR of tobacco plants to Pto DC3000 infection
- Alterations at the cellular level include: loss of membrane integrity and nuclei
- Alterations also include DNA degradation and changes in nuclease profiles

### Abstract

Light modulates almost every aspect of plant physiology, including plant-pathogen interactions. Among these, the hypersensitive response (HR) of plants to pathogens is characterized by a rapid and localized programmed cell death (PCD), which is critical to restrict the spread of pathogens from the infection site. The aim of this work was to study the role of light in the interaction between *Pseudomonas syringae* pv. *tomato* DC3000 (Pto DC3000) and non-host tobacco plants. To this end, we examined the HR under different light treatments (white and red light) by using a range of well-established markers of PCD. The alterations found at the cellular level included: i) loss of membrane integrity and nuclei, ii) RuBisCo and DNA degradation, and iii) changes in nuclease profiles and accumulation of cysteine proteinases. Our results suggest that red light plays a role during the HR of tobacco plants to Pto DC3000 infection, delaying the PCD process.

Keywords: HR, light, *Pseudomonas syringae* pv. *tomato*, tobacco, PCD, nucleases.

## 1. Introduction

Light is essential for plant metabolism, modulating almost every aspect of plant physiology [1] and playing an important role in plant-pathogen interactions [2–6]. It is well-known, for example, that tomato plants exposed to red light have increased defense capability against the plant pathogen *Pseudomonas syringae* pv. *tomato* DC3000 (Pto DC3000) [2]. Also, tomato plants inoculated with *Pseudomonas cichorii* JBC1 and exposed to red and green light show enhanced resistance and up-regulated defense-related gene expression [3]. On the other hand, recent studies revealed that light is also implicated in the regulation of bacterial physiology and in the virulence process in many important plant pathogens [7–10].

Plant-pathogen interactions may be either compatible, when a pathogen causes disease in a susceptible plant, or incompatible (or non-host), when the pathogen colonizes a resistant or non-host plant [11–13]. The latter sometimes result in a hypersensitive response (HR), a programmed cell death in plants [12,13]. The bacterial plant pathogen Pto DC3000 requires inject effectors into the plant cells through type III protein secretion system to be pathogenic. These effectors into host cells contribute to disease development in susceptible plants by suppression of plant innate immunity. However, in resistant plants type III effectors can be recognized by plant resistance (R) proteins inducing effector-triggered immunity (ETI), which includes the elicitation of the HR [14]. Tobacco plants inoculated with the phytopathogen Pto DC3000 elicit a HR [15,16].

HR may also be regulated by light. In *Arabidopsis thaliana*, for example, light regulates the development of a HR through photoreceptor proteins during an incompatible interaction [5,17,18].

The HR is characterized by reactive oxygen species (ROS) production and localized programmed cell death (PCD), the latter of which is critical to restrict the spread of pathogens from the infection site [19,20]. PCD involves several biochemical and intracellular structural changes such as the formation of apoptotic bodies, cytoplasm shrinkage, nuclear condensation and membrane blebbing [21], as well as progressive loss of RuBisCo stability [22]. Another characteristic described in PCD is specific genomic DNA cleavage, which results in a DNA ladder as a consequence of an internucleosomal DNA fragmentation into the multiples of 180 bp [21,23]. DNA ladders during cell death have also been reported in plants exposed to a pathogen toxin [21].

In PCD, DNA hydrolysis is catalyzed by nucleases (deoxyribonucleases and ribonucleases) [24], which are classified as endonucleases or exonucleases according to their enzymatic

properties [24,25]. Endonucleases, whose optimal activity depends on the pH [25], are capable of digesting double-stranded DNA (dsDNA) and are classified as  $Zn^{2+}$ -dependent or  $Ca^{2+}$ -dependent, according to their catalytic cations [24]. Several researchers have described nuclease activity in plant cells undergoing PCD [24,26–28]. Mittler and Lam (1997) [26], for example, reported that the HR:PCD response in tobacco plants is accompanied by the induction of at least four different nucleases.

Cysteine proteinases (Cys-EPs), enzymes involved in a variety of proteolytic functions in higher plants, also seem to play a role in HR:PCD [29–32]. Del Pozo and Lam (1998) [29], for example, reported Cys-EP activity during the onset of HR in the interaction between tobacco plants and tobacco mosaic virus (TMV). Some Cys-EPs present a specific KDEL motif in the C-terminal position, which is a signal for protein retention in the endoplasmic reticulum that allows the storage of Cys-EP propeptides either in small vesicles called ricinosomes [33] or in KDEL vesicles. These propeptides are then transported to vacuoles through a route which does not involve the Golgi complex [34]. Beyene et al. (2016) [31] reported the sequence of papain-like Cys-EPs in tomato leaves and suggested that this sequence is KDEL-tailed and could be involved in PCD.

The aim of the present study was to evaluate the effects of white and red light on the non-host interaction between Pto DC3000 and tobacco plants. For that purpose, we analyzed the development of symptoms caused by the bacterium and key characteristics of the PCD process, including tissue integrity, changes in cell ultrastructure, nuclear fragmentation, nuclease activity and Cys-EP accumulation. Likewise, we describe for the first time the morphological changes that occur in the nuclei, and the nuclei disassembly, both facts associated with the increase in  $Ca^{2+}$ -dependent nuclease activities in tobacco plants infiltrated with Pto DC3000 following exposure to different light conditions.

## 2. Material and methods

### 2.1. Plant material and plant inoculations

Tobacco plants (*Nicotiana tabacum* cv. Petit Havana) were used as non-host plants for Pto DC3000 [35]. The Pto DC3000 strain was grown aerobically at 28 °C with shaking at 200 rpm in King's B medium (KB) [36] containing rifampicin (Rif) 50 µg/mL. Plants were placed in a growth chamber under incandescent light at 25 °C with a photoperiod of 16-8 h light/dark. For the assays, 4-week-old tobacco plants were inoculated with a bacterial suspension containing 10<sup>8</sup> colony forming units (CFU)/mL. Bacterial suspensions were infiltrated into the intercellular spaces of fully expanded leaves by using needleless syringes. Tobacco leaves were mock infiltrated with distilled water as controls.

To test different light conditions, infiltrated plants were incubated under: i) white light with light intensity of 20 µE/m<sup>2</sup>s<sup>1</sup> provided by a fluorescent lamp (cool daylight), ii) red light with light intensity of 40 µE/m<sup>2</sup>s<sup>1</sup> provided by LEDs (630 nm) or iii) normal photoperiod (NP) (plants were grown in a greenhouse with a photoperiod of 16 h light = 150 µE/m<sup>2</sup>s<sup>1</sup>, and 8 h dark) and the symptoms caused by the bacterium were recorded up to 96 hours post-infiltration (hpi). Incubation in the dark condition was performed by covering the leaves with a black envelop. In adult plants, the growth assays were performed by grinding 0.8-cm-diameter leaf discs from Pto DC3000-infiltrated leaves at 0, 6, 16, 24, 48, 72 and 96 hpi. The discs were ground in 100 µL of 10 mM MgCl<sub>2</sub> and bacterial counts were determined by plating serial dilutions onto KB-agar plates supplemented with Rif. Colonies were counted after 48 h incubation at 28 °C. Plant bioassays were conducted three times [37].

## **2.2. Conductivity tests**

To determine electrolyte leakage, tobacco leaves were infiltrated with Pto DC3000 and exposed to white light, red light and normal photoperiod. At 6, 16, 24, 48 and 72 hpi, 0.8-cm-diameter leaf discs were collected from the inoculated areas and washed with distilled water for 30 min. Discs were then placed in microtubes with 1 mL of distilled water; next, conductivity was measured after 30 min of soaking, by using a Compact conductivity meter B-771 (LAQUAtwin). Finally, samples were destroyed by autoclaving and the conductance of boiled leaf discs was taken as 100 % ion content according to Daurelio et al. (2009) [37]. The assay was conducted three times.

## **2.3. DNA isolation and analysis**

For DNA isolation and analysis, genomic DNA was isolated from 100 mg fresh leaves infiltrated with Pto DC3000 and exposed to different light conditions for 48 h using the DNeasy plant mini kit (Qiagen, Germany). The yield and quality of the DNA obtained were assessed in a Nanodrop 2000 spectrophotometer (Thermo Fisher Scientific, MA, USA). For DNA fragmentation analysis, 2.5 µg of each sample was separated on a 0.8 % (w/v) agarose gel and stained with ethidium bromide (final concentration: 0.5 µg/mL) [27]. A GeneRuler™ 50-bp Ladder (Fermentas, MA, USA) was used as a reference. The experiment was repeated three times, with similar results in all cases.

## **2.4. Sample preparation for histological analysis**

For immunohistological and TUNEL analysis, samples of tomato plants infiltrated with Pto DC3000 and exposed to white and red light for 6 h were collected and fixed in 4 % (v/v) paraformaldehyde prepared in 0.1 M phosphate buffered saline (PBS) pH 7.2 for 24 h at 4 °C. After rinsing, samples were dehydrated in an ethanol series, and then embedded in LRW resin (Polyscience Inc., Warrington, PA, USA). Semi-thin sections were obtained with a microtome and mounted on glass slides. The sections were either stained with 0.5 % (w/v) toluidine blue O (Sigma–Aldrich, St. Louis, MO, USA) in aqueous solution or used without staining.

### **2.5. Sample preparation for subcellular analysis by transmission electron microscope (TEM)**

For subcellular analysis by TEM, samples of tomato plants infiltrated with Pto DC3000 and exposed to white and red light for 16 h were collected, fixed overnight at 4 °C in 2.5 % (v/v) glutaraldehyde in 0.1 M phosphate buffer, pH 7.2, and post-fixed in 0.5 % (w/v)  $\text{OsO}_4$  for 1 h. Then, the samples were dehydrated in an ethanol series and embedded in Spurr's resin (Sigma-Aldrich, St. Louis, MO, USA) according to Harris et al. (1995). Ultra-thin sections were mounted on grids coated with Formvar (Polyscience, Warrington, PA, USA), and stained in uranyl acetate followed by lead citrate from EMS (Hatfield, PA, USA). The sections were examined in a Zeiss M109 turbo (Zeiss, Wiesbaden, Germany) TEM operating at an accelerating voltage of 90 kV.

### **2.6. Protein extraction and quantification**

Total protein extracts were prepared by grinding Pto DC3000-infiltrated tobacco leaves exposed to different light treatments for 16 and 48 h in liquid nitrogen. The resulting powder was suspended in 50 mM Tris-HCl, pH 7.5, 5 mM MgCl<sub>2</sub>, 1 mM EDTA, and 1 mM phenylmethylsulfonyl fluoride (PMSF). For in-gel nuclease activity assays, proteins were extracted using an extraction buffer containing: 50 mM Tris-HCl, pH 7.5, 2 mM 1,4-dithiothreitol, and 0.5 mM PMSF.

Protein concentrations were determined as described by Bradford (1976) [38], using a Quick Start Bradford Protein Assay Kit 1 (Bio-Rad Laboratories, Hercules, CA, USA) and bovine serum albumin (BSA) as a standard (Bio-Rad Laboratories, Hercules, CA, USA). The assay was conducted at least three times.

## **2.7. Western Blot analysis of RuBisCo and Cys-EPs**

RuBisCo levels were determined by Western Blot analysis using polyclonal anti-RuBisCo rabbit antibody (1:4000) (kindly provided by J. J. Guiamet, Universidad Nacional de La Plata, Argentina) as described in Lopéz-Fernández et al. (2015) [27]. An aliquot of 10 µL of protein extracts were loaded onto a polyacrylamide gel to perform a Western Blot analysis. Likewise, the Cys-EP levels were determined using primary antibody raised against purified 35 kDa Cys-EP, anti-RcCys-EP, [33] and performed as described by Lopéz-Fernández et al. 2013 [39]. Briefly, 14 µg of protein extracts were loaded onto polyacrylamide gel and transferred to nitrocellulose membrane (GE Healthcare, Life Science). Primary antibodies were diluted 1:3000 in 1 % (w/v) BSA in TTBS for 2 h at room temperature.

Finally, the membranes were incubated with a secondary alkaline phosphatase-conjugated goat anti-rabbit antibody (Sigma A3587, Merck KGaA, Darmstadt, Germany) diluted 1:5000

in TTBS for 1:30 h at room temperature. Signal was detected with NBT/BCIP solution (Promega, Madison, WI, USA). Western Blot analyses were repeated at least three times on independent biological samples, and representative results are shown.

## **2.8. *In situ* immunolocalization of RuBisCo**

RuBisCo was *in situ* immunolocalized as described in López-Fernández et al. (2015) [27]. Sections were incubated overnight with rabbit anti-RuBisCo diluted 1:200. As controls, sections were treated as above but excluding anti-RuBisCo antiserum. Sections were then incubated with 5 nm diameter colloidal gold-conjugated goat antiserum raised to rabbit immunoglobulins (Merck KGaA, Darmstadt, Germany) diluted 1:200 in PBST plus 0.1 % BSA. After 10 min fixation with 2.5 % glutaraldehyde in 0.1M PBS, pH 7.2, sections were thoroughly washed with Milli-Q-grade water. Finally, the sections were treated with silver enhancer, and contrasted in 0.1 % toluidine blue O (Sigma–Aldrich) in aqueous solution. Each image is a representative result of observation of at least five semi-thin sections of tobacco leaves exposed to the different light treatments.

## **2.9. TUNEL assay**

*In situ* DNA fragmentation was detected by the terminal deoxyribonucleotidyl transferase (TdT)-mediated biotin-dUTP nick-end labeling (TUNEL) assay (*In situ* cell detection kit TMR red; Merck KGaA, Darmstadt, Germany), performed according to the protocol provided by the manufacturer. Negative controls were included by omitting the TdT enzyme from the reaction mixture. To obtain positive controls, sections were incubated with DNase I (image not shown) prior to the TUNEL reaction. Images were obtained by Axioskop 2

microscope (Carl Zeiss, Jena, Germany), captured with an EOS 1000D camera (Carl Zeiss, Jena, Germany), and compiled with Photoshop version CS6 (Adobe systems). DAPI filters (excitation 340–390 nm, emission 420–470 nm) and rhodamine filters (excitation 540–552 nm, emission 575–640 nm) were used to examine samples by the TUNEL assay. At least five semi-thin sections of each treatment were observed.

### **2.10. *In-gel* nuclease activity assay**

DNase and RNase activity assays were performed according to López-Fernández et al. (2018) [40]. Protein extracts (20 µg) from tobacco leaves exposed to white and red light for 16 and 48 h were loaded on 12 % SDS-PAGE containing herring sperm DNA (Biodynamics, Argentina) or torula yeast RNA (Merck KGaA, Darmstadt, Germany). For single-stranded DNase activity assays, DNA was boiled for 5 min prior to pouring in the resolving gels. The gels were washed in a buffer containing 25 % 2- propanol and 1 mM EDTA. Subsequently, the gels containing DNA or RNA were incubated either overnight (DNA) at 37 °C or for 2 h (RNA) at 50 °C, in 10 mM Tris–HCl neutral buffer (pH 8.0, containing 10 mM CaCl<sub>2</sub>, 0.2 mM DTT and 1 % [v/v] Triton X-100). After incubations, the gels were washed three times for 5 min in buffer (10 mM Tris–HCl pH 8.0, 1 mM EDTA). The gels were stained with 0.01 mg/mL ethidium bromide and photographed. All SDS-PAGE results were replicated at least three times and similar results were obtained.

### **2.11. Statistical analysis**

Descriptive statistics were analyzed by one-way ANOVA and differences between treatments were determined following Tukey's HSD post-hoc test, at  $p \leq 0.05$ . The plotted

data correspond to the average of these independent determinations, with the corresponding standard error indicated by the error bars.

### **3. Results**

#### **3.1. Light affected HR response in tobacco leaves infiltrated with Pto DC3000**

As mentioned above, to evaluate the effect of light on the non-host response, tobacco plants were infiltrated with Pto DC3000 ( $10^8$  CFU/mL) and exposed to white, red light and normal photoperiod (NP). The plant symptoms were analyzed up to 96 hpi. Tobacco leaves exposed to white light presented typical HR lesions, which became evident at 16 hpi, whereas those exposed to red light presented no symptoms until 48 hpi. Although plants exposed to NP and to white light showed similar development of HR lesions at 16 hpi, the severity of the necrosis in leaves exposed to white light was higher after 48 hpi compared to NP treatment (Fig. 1A). Bacterial growth was also analyzed by monitoring the number of bacterial cells. As shown in Fig. 1B, the number of bacterial cells recovered from leaves exposed to white light and normal photoperiod began to decrease after 24 hpi, and the number of recovered bacteria at 72 and 96 hpi was significantly lower than that recovered from leaves exposed to red light at the same times. The number of bacterial cells recovered between 24 and 72 hpi from leaves exposed to red light remained almost constant and then started to decrease.

#### **3.2. Electrolyte leakage was lower in leaves exposed to red light than in those exposed to white light**

Electrolyte leakage was measured to estimate the degree of cell membrane injury produced by Pto DC3000. At all times evaluated (6, 16, 24, 48 and 72 hpi), membrane permeability

showed an increase in leaves exposed to white light and normal photoperiod. Membrane permeability also showed an increase in leaves exposed to red light respect to controls in all times. The ion leakage values remained constant after 24 hpi in leaves exposed to all light treatments (Fig. 1C). These results suggest a greater effect of white light and NP treatments respect to red light treatment.

### **3.3. Leaves exposed to red light showed less RuBisCo loss than those exposed to white light**

RuBisCo accumulation in Pto DC3000-infiltrated tobacco leaves exposed to white light, red light and dark conditions for 6 h was studied using a rabbit polyclonal anti-RuBisCo antiserum by *in situ* immunolocalizations. A markedly decrease in RuBisCo content was observed in dark condition (Fig. 2A)

The Western Blot allowed detecting the large subunit of RuBisCo by showing bands at molecular mass of approximately 53 kDa. Leaves exposed to white and dark treatments presented reduction in RuBisCo accumulation (Fig. 2B).

A Coomassie-stained gel was simultaneously performed (Fig. 2B), and, as expected, the RuBisCo quantity observed was consistent with that detected by the Western Blot analysis.

Plants kept in the dark showed a marked decrease in the RuBisCo content.

To analyze PCD, genomic DNA was isolated from leaves exposed to the different light conditions and separated by agarose gel electrophoresis (Fig. 3A). When exposed to white light, extensive internucleosomal DNA fragments of multiples of approximately 200 bp were detected, indicating degradation of DNA. In contrast, lower amounts were observed when exposed to red light. Some degree of DNA degradation was observed in plants placed in the dark.

To evaluate *in situ* detection of DNA damage, a TUNEL assay was performed. Fig. 3C shows representative TUNEL assay images from tobacco leaf sections infiltrated with Pto DC3000 and exposed to white and red light. TUNEL-positive signals were detected in both light treatments, whereas in control leaves the nuclei were TUNEL-negative. Leaves exposed to white light presented a greater number of affected nuclei than those treated with red light (Fig. 3C). The percentage of labeled nuclei in leaves exposed to white light was 57 %, whereas that in those exposed to red light was 30 %. Positive control treatments were conducted for each set of slides (data not shown).

Initially, nuclei were round with a clear nuclear envelope (Fig. 3B(a) and 4A), whereas as the nuclear disassembly started, chromatin condensation into discrete patches distributed throughout the nucleus as well as nuclear shrinkage were observed (Fig. 3B(c-d), 4B). In this state, the nucleus i) was discharged and enclosed in the central vacuole as a whole organelle by autophagy following an incomplete PCD (Fig. 4C) or ii) completed the PCD program without going through autophagy (Fig. 3B(d)).

#### **3.4. Light induced the activity of different nucleases during the PCD process caused by HR in tobacco leaves**

To examine the effect of Pto DC3000 infection and different light exposure treatments on the activity of nucleases and ribonucleases in leaves, an in-gel nuclease activity assay was performed. Figure 5 shows the DNA-RNA SDS-PAGEs used to identify the activities of the DNases and RNases (Fig. 5A) and total protein content (Fig. 5B) in the different light treatments. When dsDNA was used as substrate, the assay revealed the presence of five  $\text{Ca}^{2+}$ -dependent nucleases at 16 hpi: n15, n24, n75, n56 and n43. n15 was active only in leaves

exposed to red light, whereas n75 and n24 were active only in leaves exposed to white light and red light. n56 and n43 showed no differences in their activity between the treatments and control. At 48 hpi the assay revealed the presence of six Ca<sup>2+</sup>-dependent nucleases n31, n20, n75, n34, n56 and n43. n31 and n20 showed higher nuclease activity in leaves exposed to white light, whereas n75 were active only in leaves exposed to white light and red light, when internucleosomal DNA fragmentation became evident. Likewise, n56, n43 and 34 showed no differences in their activity between the treatments and control. We also examined the metal ion specificity for the nuclease activity and found that all the nucleases were activated in the presence of the Ca<sup>2+</sup> ion (Fig. 5A).

When RNA was used as substrate, at 48 hpi two bands of molecular masses of 10 and <10 kDa were revealed. In leaves exposed to white light, the nuclease of molecular mass 10 kDa increased its activity, whereas that of molecular mass <10 kDa had the lowest activity (Fig. 5A). No activity was detected at 16 hpi (Supp Fig.1). Determination of nuclease activity in tobacco leaves infiltrated with Pto DC3000 and exposed to normal photoperiod showed the same nuclease activation pattern of plants exposed to white light (Supp Fig.1). At 48 hpi the protein content was different between light treatments and control (Fig. 5B).

### 3.5. Light affected Cys-EP accumulation in Pto DC3000-infiltrated tobacco leaves

To characterize the accumulation of Cys-EPs during HR in tobacco leaves exposed to white and red light, a Western Blot using an anti-RcCys-EP antibody was performed. The Western Blot analysis showed the presence of the Cys-EP mature form (35-kDa band), which reached its highest levels in leaves exposed to white light. The accumulation of Cys-EPs in leaves exposed to red light was lower than that in those exposed to white light (Fig. 6A). A

Coomassie stained SDS-PAGE was performed separately to ensure equal protein loading (Fig. 6B).

#### 4. Discussion

Plants have evolved defense mechanisms against pathogens like bacteria, viruses and fungi. Following pathogen attack, in an avirulent plant-pathogen interaction, plants can detect the pathogen and trigger a HR [41,42], which is a localized plant-defense mechanism that triggers PCD to restrict the spread of pathogens from the infection site [43,44].

Some authors have reported that plant responses to pathogen invasion are markedly different depending on the light treatment applied [5,17,18], and it is well-known that the HR in plants is affected by light [5,17,18,45]. Also, previous studies have indicated that phytopathogen bacteria are able to sense light and regulate some physiological processes such as, motility, attachment and virulence in response to light [7–10]. Bacteria perceive light through photosensory proteins, detecting different wavelengths. In *Pseudomonas syringae* pv. tomato DC 3000 genome three photoreceptors have been identified: two red light (bacteriophytochromes) and one blue light (LOV type protein) [7,9]. However, the mechanisms of how pathogens exploit light signals to promote virulence and plant infection are not fully understood yet.

The role of light in the plant-pathogen interaction has been focused mainly on compatible interaction [7-9]. In this work, we demonstrated that red light delayed the appearance of HR-induced symptoms in the incompatible interaction between Pto DC3000 and tobacco plants. Cell death associated with the HR in plants generates cellular collapse and local lesions [44,46]. In this study, we demonstrated that the characteristic symptoms induced by the HR,

i.e. a brown and dried necrotic area in the infection site, in Pto DC3000-infiltrated tobacco leaves exposed to red light appeared delayed (Fig. 1A). Also, the number of bacteria recovered from leaves exposed to red light remained practically constant (approximately  $10^7$  CFU/cm<sup>2</sup>) (Fig. 1B).

Our results showed a light effect in the growth behavior of Pto DC3000 and tobacco plants, as previously reported by Zeier et al., (2004) [18], with *Pseudomonas syringae* pv. *maculicola* during the incompatible interaction with *Arabidopsis* plants.

During the course of HR, the cellular membrane system is subjected to irreversible damage, being ROS production and fatty acid and lipid peroxidation the main generators for increased membrane deterioration [47]. Measurement of electrolyte leakage has also been previously related to cell death [40,48]. In this study, membrane deterioration was higher in Pto DC3000-infiltrated leaves exposed to white light and normal photoperiod (Fig. 1C).

Nuclear DNA fragmentation is induced by the PCD triggered by biotic stress in plants [21,26,41]. The TEM images here obtained, accompanied by the ladder analysis (Fig. 3), proved that nuclei from leaves exposed to white and red light showed a PCD nuclear disassembly pattern. The TEM images also evidenced that nuclei were delivered to vacuoles for degradation, following an autophagic route, a mechanism that controls HR:PCD [42,49] (Fig. 4). Coll et al. (2014) [50] demonstrated that both autophagy and AtMC1, a plant metacaspase that plays a role as a positive regulator of pathogen-triggered PCD, are part of parallel pathways, both positively regulating HR cell death in young plants.

The characteristic DNA ladder of multiples of ca. 180–200 bp arises as a consequence of internucleosomal DNA fragmentation due to endonuclease activities [21,23,27,51]. Mittler et al. (1997) [26] detected DNA degradation during HR cell death in tobacco leaves infected with TMV and *Pseudomonas syringae* pv. *phaseolicola* at 24 and 48 hpi. Here, DNA

fragmentation was evaluated in Pto DC3000-infiltrated tobacco leaves exposed to different light conditions, at 48 hpi by agarose electrophoresis and at 6 hpi by TUNEL, to detect the first signs of strand breaks. In leaves exposed to red light, only a few nuclei showed TUNEL-positive labeling and some degree of DNA laddering was evident, whereas in leaves exposed to white light, the number of labelled nuclei was significantly higher and the DNA laddering was noticeably more evident than in plants exposed to red light (Fig. 3A and 3C). These results demonstrate that red light delays the programmed nuclear disassembly process in tobacco leaves infiltrated with Pto DC3000. In control leaves, the electrophoretic run showed little DNA smearing (Fig. 3A), which is mostly attributable to a normal PCD process and may be the result of the presence of parenchyma, xylem and phloem cells that may undergo an independent PCD [26]. According to Lambert et al (2017) [28] and Blank and McKeon (1989) [52] dark-induced senescence caused a marked decrease in the chlorophyll, total soluble protein and putative RuBisCO, and also DNA degradation. In this work some DNA degradation and lower content of RuBisCO was evident for plant kept in darkness (Figs 2 and 3). Coinciding with those authors, we attribute our results to the onset of induced senescence.

Plants have two major classes of endonucleases active towards dsDNA: Zn<sup>2+</sup>-dependent and Ca<sup>2+</sup>-dependent endonucleases [24]. During the HR in plants, Ca<sup>2+</sup> cytosolic levels increase, a fact that has been observed in several plant species, such as tobacco, *Arabidopsis*, soybean, and rice [53,54]. Mittler and Lam (1995) [55] reported the existence of HR-associated nucleases that may participate in DNA degradation during the HR:PCD in tobacco leaves and that these nuclease activities were stimulated by Ca<sup>2+</sup> and inhibited by EGTA, EDTA, and Zn<sup>2+</sup>. Kaneda et al. (2009) [54] reported that an endonuclease called IREN, which contains a Ca<sup>2+</sup>-binding site in the C-terminal region, is involved in the DNA fragmentation

in HR:PCD in cultured rice cells. Here, the induction of nuclease activities was tested at different light conditions following activation of HR cell death. All dsDNA nuclease activities reported were stimulated by  $\text{Ca}^{2+}$ . The 15 kDa (n15), 20 kDa (n20), 24 kDa (n24), 31 kDa (n31) and 75 kDa (n75) nucleases were active under white and red lights. This finding suggests that are HR-associated nucleases. The nuclease of 31 kDa (n31) and the ribonuclease of 10 kDa (n10) revealed higher activities under white light. This increase in nuclease activities was coordinated with a marked DNA cleavage into internucleosomal fragments, which were revealed by agarose electrophoresis. The other nucleases here observed in our light treatments and controls might be the result of Pto DC3000 infiltration, as reported previously by Mittler et al. (1997) [26] (Fig 5).

Between plants under white light and normal photoperiod treatments no differences in the growth curves of Pto DC3000, electrolyte leakage, and nuclease activity were found.

Other enzymes involved in bacterial cell wall growth are peptide hydrolases (peptidases and proteases), which can be classified into endopeptidases, which cleave on the interior of peptide chains, and exopeptidases, which cleave peptide bonds on termini of peptide chains. This classification is based on the kind of active site residue, e.g. cysteine-, serine-, aspartic-, or metallo types, and not on the substrate type [56]. Cysteine endopeptidases (Cys-EPs) are involved in different processes in plants, including PCD [57]. According to Schmid et al. (1998) [33], Cys-EPs are members of a papain family of Cys-EPs, and according to previous reports, cysteine proteinases belonging to the papain family are involved in both compatible and incompatible plant-pathogen interactions [57,58]. In *Nicotiana benthamiana*, for example, deficiency of cathepsin B, a papain-like cysteine protease that positively regulates HR, has been found to restrict the PCD triggered by *Erwinia amylovora* and *P. syringae* [58]. Also, a Cys-EP from *R. communis* has been found to bind to a Cys-EP expressed in

ricinosomes and appears as a pro-enzyme of 45 kDa and as a single 35-kDa band which corresponds to the mature form [59]. In this work, the mature form of this Cys-EP (35 kDa) was detected in all conditions at 48 hpi, but, in leaves exposed to white light its levels were higher than in those exposed to red light (Fig. 6).

In conclusion, the results of the present study add knowledge about the regulation of HR:PCD in tobacco plants infected with Pto DC3000 under different light treatments and demonstrate that red light delays the PCD process during HR. This study provides a starting point for future research aiming to identify the light-sensing mechanisms and the pathways involved in the PCD process during HR in plants.

#### **Author contributions**

Conceived and designed the experiments: EGO, SM, LM, MP L-F. Performed the experiments: LM, MP L-F, AC, JMN, SP. Performed the data analysis: LM, MP L-F, EGO, SM. Contributed reagents/materials/ analysis tools: SM, EGO, MP L-P. Wrote the first draft of the paper: SM, LM, MP L-F. All authors contributed to discussing the results and editing the paper.

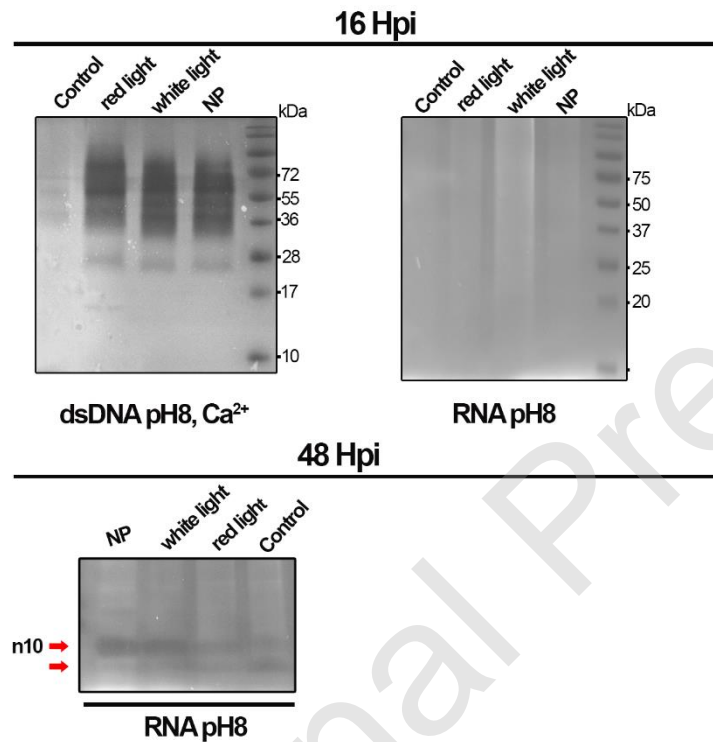
#### **Funding**

This work was supported by Agencia Nacional de Promoción Científica y Tecnológica, (PICT 2014-2487 to EGO), Universidad de Buenos Aires (UBACYT 20020100100232 to SM) and Consejo Nacional de Investigaciones Científicas y Técnicas (CONICET. Res. 7879/14 IA to ML-F and 810/13.P IP 0465 to SM), Argentina. The funders had no role in study design, data collection and analysis, decision to publish, or preparation of the manuscript.

## Conflict of interest

The authors declare that there is no conflict of interests.

## Supplementary material



**Supp Fig.1.** Determination of nuclease activity in tobacco leaves infiltrated with Pto DC3000 and exposed to white, red light and normal photoperiod (NP) for 16 and 48 h by using the *in-gel* activity assay with dsDNA and RNA as substrate. Control plants were incubated under normal photoperiod. Analyses were repeated at least three times on independent biological samples, and representative results are shown.

**References**

- [1] C.L. Ballaré, Light regulation of plant defense, *Annu. Rev. Plant Biol.* 65 (2014) 335–363. doi:10.1146/annurev-arplant-050213-040145.
- [2] Y. Yang, M. Wang, Y. Yin, E. Onac, G.-F. Zhou, S. Peng, X. Xia, K. Shi, J. Yu, Y. Zhou, RNA-seq analysis reveals the role of red light in resistance against *Pseudomonas syringae* pv. *tomato* DC3000 in tomato plants, *BMC Genomics*. 16 (2015) 120. doi:10.1186/s12864-015-1228-7.
- [3] R. Nagendran, Y.H. Lee, Green and red light reduces the disease severity by *Pseudomonas cichorii* JBC1 in tomato plants via upregulation of defense-related gene expression, *Phytopathology*. 105 (2015) 412–418. doi:10.1094/PHYTO-04-14-0108-R.
- [4] T. Griebel, J. Zeier, Light regulation and daytime dependency of inducible plant defenses in *Arabidopsis*: phytochrome signaling controls systemic acquired resistance rather than local defense, *PLANT Physiol.* 147 (2008) 790–801. doi:10.1104/pp.108.119503.
- [5] A.C. Chandra-Shekara, M. Gupte, D. Navarre, S. Raina, R. Raina, D. Klessig, P. Kachroo, Light-dependent hypersensitive response and resistance signaling against Turnip Crinkle Virus in *Arabidopsis*, *Plant J.* 45 (2006) 320–334. doi:10.1111/j.1365-313X.2005.02618.x.
- [6] M.R. Roberts, N.D. Paul, Seduced by the dark side: integrating molecular and ecological perspectives on the influence of light on plant defence against pests and pathogens, *New Phytol.* 170 (2006) 677–699. doi:10.1111/j.1469-8137.2006.01707.x.
- [7] I. Kraiselburd, L. Moyano, A. Carrau, J. Tano, E.G. Orellano, Bacterial photosensory proteins and their role in plant-pathogen interactions, *Photochem. Photobiol.* 93 (2017) 666–674. doi:10.1111/php.12754.
- [8] R. McGrane, G.A. Beattie, *Pseudomonas syringae* pv. *syringae* B728a regulates multiple stages of plant colonization via the bacteriophytochrome BphP1, *MBio*. 8 (2017) 1–16. doi:10.1128/mBio.01178-17.
- [9] S. Santamaría-Hernando, J.J. Rodríguez-Herva, P.M. Martínez-García, I. Río-Álvarez, P.

- González-Melendi, J. Zamorano, C. Tapia, P. Rodríguez-Palenzuela, E. López-Solanilla, *Pseudomonas syringae* pv. *tomato* exploits light signals to optimize virulence and colonization of leaves, *Environ. Microbiol.* 20 (2018) 4261–4280. doi:10.1111/1462-2920.14331.
- [10] N. Rajalingam, Y.H. Lee, Effects of green light on the gene expression and virulence of the plant pathogen *Pseudomonas cichorii* JBC1, *Eur. J. Plant Pathol.* 150 (2018) 223–236. doi:10.1007/s10658-017-1270-1.
- [11] S.T. Chisholm, G. Coaker, B. Day, B.J. Staskawicz, Host-microbe interactions: shaping the evolution of the plant immune response, *Cell.* 124 (2006) 803–814. doi:10.1016/j.cell.2006.02.008.
- [12] M.C. Heath, Nonhost resistance and nonspecific plant defenses, *Curr. Opin. Plant Biol.* 3 (2000) 315–319. doi:10.1016/S1369-5266(00)00087-X.
- [13] L.A.J. Mur, P. Kenton, A.J. Lloyd, H. Ougham, E. Prats, The hypersensitive response; the centenary is upon us but how much do we know?, *J. Exp. Bot.* 59 (2008) 501–520. doi:10.1093/jxb/erm239.
- [14] M. Guo, F. Tian, Y. Wamboldt, J.R. Alfano, The majority of the type III effector inventory of *Pseudomonas syringae* pv. *tomato* DC3000 can suppress plant immunity, *Mol. Plant-Microbe Interact.* 22 (2009) 1069–1080. doi:10.1094/MPMI-22-9-1069.
- [15] J.R. Alfano, A. Collmer, Bacterial pathogens in plants: life up against the wall, *Plant Cell.* 8 (1996) 1683. doi:10.2307/3870222.
- [16] G.M. Preston, *Pseudomonas syringae* pv. *tomato*: the right pathogen, of the right plant, at the right time, *Mol. Plant Pathol.* 1 (2000) 263–275. doi:10.1046/j.1364-3703.2000.00036.x.
- [17] T. Genoud, A.J. Buchala, N. Chua, J.-P. Métraux, Phytochrome signalling modulates the SA-perceptive pathway in *Arabidopsis*., *Plant J.* 31 (2002) 87–95. <http://www.ncbi.nlm.nih.gov/pubmed/12100485>.
- [18] J. Zeier, B. Pink, M. Mueller, S. Berger, Light conditions influence specific defence responses

- in incompatible plant-pathogen interactions: uncoupling systemic resistance from salicylic acid and PR-1 accumulation, *Planta*. 219 (2004) 673–683. doi:10.1007/s00425-004-1272-z.
- [19] K.S. Mysore, C.-M. Ryu, Nonhost resistance: how much do we know?, *Trends Plant Sci.* 9 (2004) 97–104. doi:10.1016/j.tplants.2003.12.005.
- [20] V. Nurnberger, Thorsten and Lipka, Non-host resistance in plants: new insights into an old phenomenon, *Mol. Plant Pathol.* 6 (2005) 335–345. doi:10.1111/J.1364-3703.2004.00279.X.
- [21] A. Danon, V. Delorme, N. Mailhac, P. Gallois, Plant programmed cell death: A common way to die, *Plant Physiol. Biochem.* 38 (2000) 647–655. doi:10.1016/S0981-9428(00)01178-5.
- [22] H. Li, P.H. Goodwin, Q. Han, L. Huang, Z. Kang, Microscopy and proteomic analysis of the non-host resistance of *Oryza sativa* to the wheat leaf rust fungus, *Puccinia triticina* f. sp. *tritici*, *Plant Cell Rep.* 31 (2012) 637–650. doi:10.1007/s00299-011-1181-0.
- [23] F. Domínguez, F.J. Cejudo, A comparison between nuclear dismantling during plant and animal programmed cell death, *Plant Sci.* 197 (2012) 114–121. doi:10.1016/j.plantsci.2012.09.009.
- [24] M. Sugiyama, J. Ito, S. Aoyagi, H. Fukuda, Endonucleases, in: *Program. Cell Death High. Plants*, Springer Netherlands, Dordrecht, 2000: pp. 143–153. doi:10.1007/978-94-010-0934-8\_11.
- [25] W. Sakamoto, T. Takami, Nucleases in higher plants and their possible involvement in DNA degradation during leaf senescence, *J. Exp. Bot.* 65 (2014) 3835–3843. doi:10.1093/jxb/eru091.
- [26] R. Mittler, L. Simon, E. Lam, Pathogen-induced programmed cell death in tobacco., *J. Cell Sci.* 110 ( Pt 1 (1997) 1333–44. <http://www.ncbi.nlm.nih.gov/pubmed/9202394>.
- [27] M.P. López-Fernández, H.P. Burrieza, A.J. Rizzo, L.J. Martínez-Tosar, S. Maldonado, Cellular and molecular aspects of quinoa leaf senescence, *Plant Sci.* 238 (2015) 178–187. doi:10.1016/j.plantsci.2015.06.003.
- [28] R. Lambert, F.A. Quiles, G. Gálvez-Valdivieso, P. Piedras, Nucleases activities during

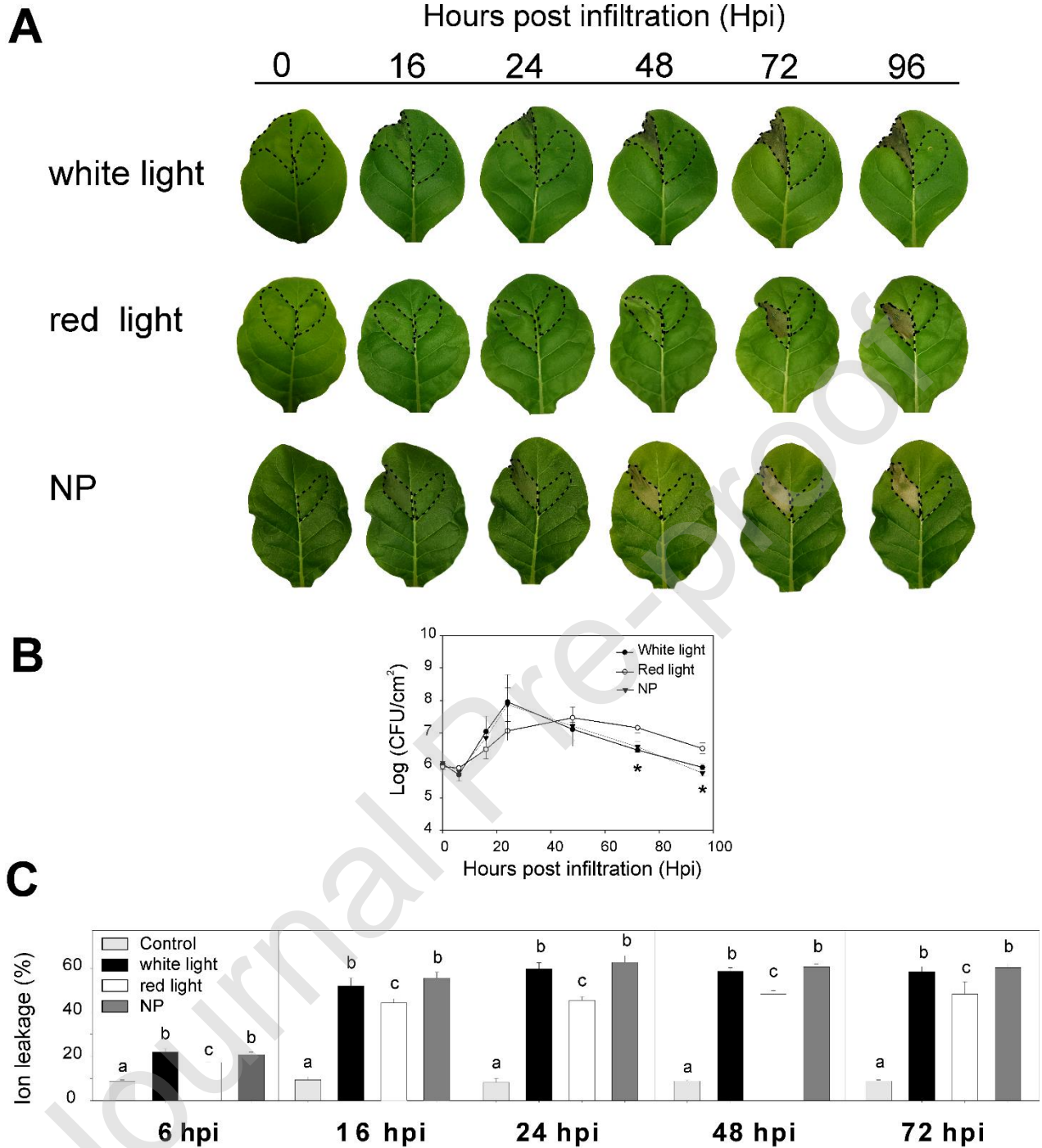
- French bean leaf aging and dark-induced senescence, *J. Plant Physiol.* 218 (2017) 235–242. doi:10.1016/j.jplph.2017.08.013.
- [29] O. del Pozo, E. Lam, Caspases and programmed cell death in the hypersensitive response of plants to pathogens, *Curr. Biol.* 8 (1998) 1129–1132. doi:10.1016/S0960-9822(98)70469-5.
- [30] M. Elbaz, A. Avni, M. Weil, Constitutive caspase-like machinery executes programmed cell death in plant cells, *Cell Death Differ.* 9 (2002) 726–733. doi:10.1038/sj.cdd.4401030.
- [31] G. Beyene, C.H. Foyer, K.J. Kunert, Two new cysteine proteinases with specific expression patterns in mature and senescent tobacco (*Nicotiana tabacum* L.) leaves, *J. Exp. Bot.* 57 (2006) 1431–1443. doi:10.1093/jxb/erj123.
- [32] G.S. Salvesen, A. Hempel, N.S. Coll, Protease signaling in animal and plant-regulated cell death, *FEBS J.* 283 (2016) 2577–2598. doi:10.1111/febs.13616.
- [33] M. Schmid, D. Simpson, F. Kalousek, C. Gietl, A cysteine endopeptidase with a C-terminal KDEL motif isolated from castor bean endosperm is a marker enzyme for the ricinosome, a putative lytic compartment, *Planta.* 206 (1998) 466–475. doi:10.1007/s004250050423.
- [34] T. Okamoto, C-Terminal KDEL sequence of a KDEL-tailed cysteine proteinase (sulfhydryl-endopeptidase) is involved in formation of KDEL vesicle and in efficient vacuolar transport of sulfhydryl-endopeptidase, *PLANT Physiol.* 132 (2003) 1892–1900. doi:10.1104/pp.103.021147.
- [35] R.C. Keith, Alginate gene expression by *Pseudomonas syringae* pv. *tomato* DC3000 in host and non-host plants, *Microbiology.* 149 (2003) 1127–1138. doi:10.1099/mic.0.26109-0.
- [36] D.E.R. E. O. King, M. K. Ward, Two simple media for the demonstration of pyocyanin and fluorescein, *J. Laboratoty Clin. Med.* 44 (1954) 301–307.
- [37] O.E. Daurelio LD, Tondo ML, Dunger G, Gottig N, Ottado J, Hypersensitive Response, in: editors. In: Narwal SS, Catala'n AN, Sampietro DA, Vattuone MA, Polyticka B (Ed.), *B. Plant Bioassays Sect. II Plantmicroorganisms Interact.*, Houston: Studium Press, LLC., 2009: pp. 187–206.

- [38] M.M. Bradford, A rapid and sensitive method for the quantitation of microgram quantities of protein utilizing the principle of protein-dye binding, *Anal. Biochem.* 72 (1976) 248–254. doi:10.1016/0003-2697(76)90527-3.
- [39] M.P. López-Fernández, S. Maldonado, Ricinosomes provide an early indicator of suspensor and endosperm cells destined to die during late seed development in quinoa (*Chenopodium quinoa*), *Ann. Bot.* 112 (2013) 1253–1262. doi:10.1093/aob/mct184.
- [40] M.P. López-Fernández, L. Moyano, M.D. Correa, F. Vasile, H.P. Burrieza, S. Maldonado, Deterioration of willow seeds during storage, *Sci. Rep.* 8 (2018) 17207. doi:10.1038/s41598-018-35476-3.
- [41] M. Huysmans, S. Lema A, N.S. Coll, M.K. Nowack, Dying two deaths-programmed cell death regulation in development and disease, *Curr. Opin. Plant Biol.* 35 (2017) 37–44. doi:10.1016/j.pbi.2016.11.005.
- [42] A.Y. Leary, N. Sanguankiatichai, C. Duggan, Y. Tumtas, P. Pandey, M.E. Segretin, J. Salguero Linares, Z.D. Savage, R.J. Yow, T.O. Bozkurt, Modulation of plant autophagy during pathogen attack, *J. Exp. Bot.* 69 (2018) 1325–1333. doi:10.1093/jxb/erx425.
- [43] C. Lamb, R.A. Dixon, The oxidative burst in plant disease resistance, *Annu. Rev. Plant Physiol. Plant Mol. Biol.* 48 (1997) 251–275. doi:10.1146/annurev.arplant.48.1.251.
- [44] J. Salguero-Linares, N.S. Coll, Plant proteases in the control of the hypersensitive response, *J. Exp. Bot.* (2019). doi:10.1093/jxb/erz030.
- [45] M.L. Delprato, A.R. Krapp, N. Carrillo, Green light to plant responses to pathogens: the role of chloroplast light-dependent signaling in biotic stress, *Photochem. Photobiol.* 91 (2015) 1004–1011. doi:10.1111/php.12466.
- [46] J.G.S. Gray, J., Janick-Buckner D, Buckner B, Close P. S., Light-dependent death of maize lls1 cells is mediated by mature chloroplasts, *Plant Physiol.* 130 (2002) 1894–1907. doi:10.1104/pp.008441.
- [47] E. Kombrink, E. Schmelzer, The hypersensitive response and its role in disease resistance,

- Eur. J. Plant Pathol. 107 (2001) 69–78.
- [48] V. Demidchik, Mechanisms of oxidative stress in plants: From classical chemistry to cell biology, *Environ. Exp. Bot.* 109 (2015) 212–228. doi:10.1016/j.envexpbot.2014.06.021.
- [49] Y. Liu, M. Schiff, K. Czymbek, Z. Tallóczy, B. Levine, S.P. Dinesh-Kumar, Autophagy regulates programmed cell death during the plant innate immune response, *Cell*. 121 (2005) 567–577. doi:10.1016/j.cell.2005.03.007.
- [50] N.S. Coll, A. Smidler, M. Puigvert, C. Popa, M. Valls, J.L. Dangl, The plant metacaspase AtMC1 in pathogen-triggered programmed cell death and aging: functional linkage with autophagy., *Cell Death Differ.* 21 (2014) 1–10. doi:10.1038/cdd.2014.50.
- [51] N.S. Coll, D. Vercammen, A. Smidler, C. Clover, F. Van Breusegem, J.L. Dangl, P. Epple, Arabidopsis type I metacaspases control cell death, *Science*. 330 (2010) 1393–1397. doi:10.1126/science.1194980.
- [52] A. Blank, T. McKeon, Single-strand-preferring nuclease activity in wheat leaves is increased in senescence and is negatively photoregulated., *Proc. Natl. Acad. Sci. U. S. A.* 86 (1989) 3169–73.
- [53] A. Levine, R.I. Pennell, M.E. Alvarez, R. Palmer, C. Lamb, Calcium-mediated apoptosis in a plant hypersensitive disease resistance response, *Curr. Biol.* 6 (1996) 427–437. doi:10.1016/S0960-9822(02)00510-9.
- [54] T. Kaneda, Y. Taga, R. Takai, M. Iwano, H. Matsui, S. Takayama, A. Isogai, F.-S. Che, The transcription factor OsNAC4 is a key positive regulator of plant hypersensitive cell death, *EMBO J.* 28 (2009) 926–936. doi:10.1038/emboj.2009.39.
- [55] R. Mittler, E. Lam, Identification, characterization, and purification of a tobacco endonuclease activity induced upon hypersensitive response cell death, *Plant Cell*. 7 (1995) 1951–1962. doi:10.2307/3870202.
- [56] M. Grudkowska, B. Zagdańska, Multifunctional role of plant cysteine proteinases, *Acta Biochim. Pol.* 51 (2004) 609–624. doi:045103609.

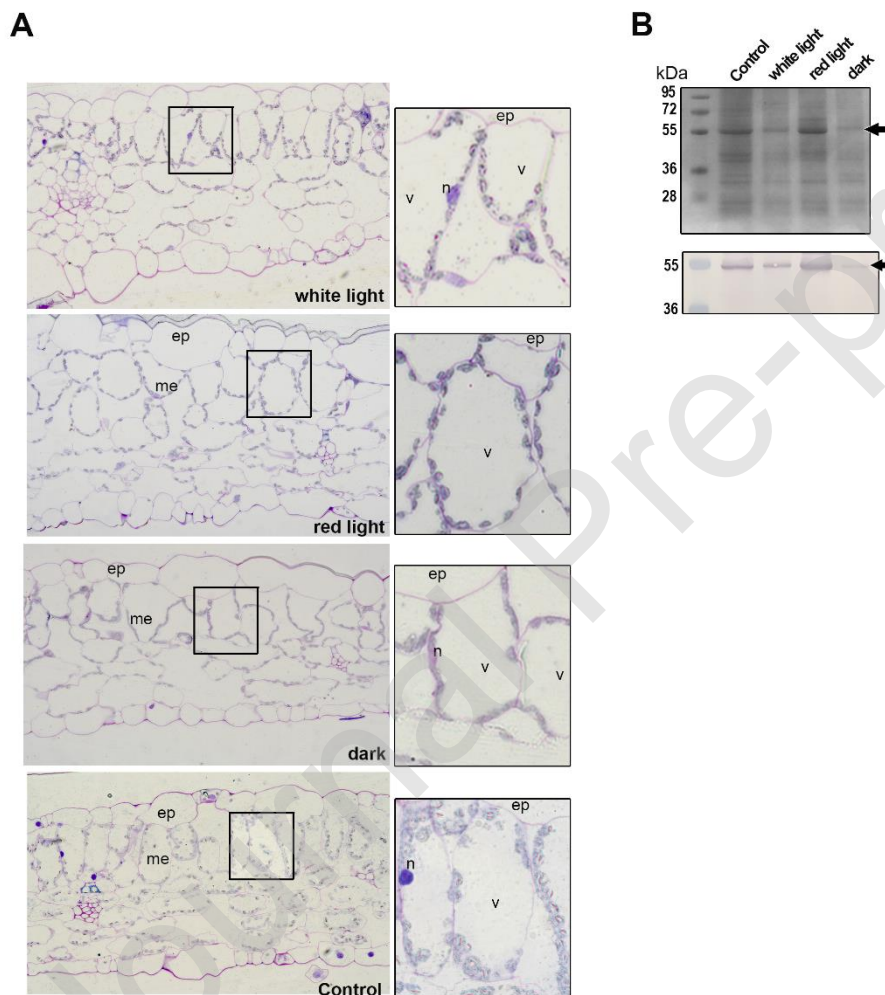
- [57] L. Hao, T. Hsiang, P.H. Goodwin, Role of two cysteine proteinases in the susceptible response of *Nicotiana benthamiana* to *Colletotrichum destructivum* and the hypersensitive response to *Pseudomonas syringae* pv. *tomato*, *Plant Sci.* 170 (2006) 1001–1009. doi:10.1016/j.plantsci.2006.01.011.
- [58] E.L. Thomas, R.A.L. van der Hoorn, Ten prominent host proteases in plant-pathogen interactions, *Int. J. Mol. Sci.* 19 (2018) 639. doi:10.3390/ijms19020639.
- [59] M.P. López-Fernández, S. Maldonado, Programmed cell death during quinoa perisperm development, *J. Exp. Bot.* 64 (2013) 3313–3325. doi:10.1093/jxb/ert170.

**Fig. 1. (A)** Representative leaves at 0, 16, 24, 48, 72 and 96 h post-inoculation (hpi) with Pto DC3000 and exposed to white light, red light and normal photoperiod (NP). Dashed lines indicate the infiltrated area. Left area: infiltrated with Pto DC3000. Right area: Control, infiltrated with distilled water. **(B)** Growth curves of Pto DC3000 in the apoplastic space of tobacco leaves exposed to white light, red light and NP. Bacterial populations in leaf tissues were determined by serial dilution and plating. **(C)** Cell membrane injuries produced by Pto DC3000 infection on tobacco leaves exposed to white light, red light and NP for 6, 16, 24, 48 and 72 hpi. Control plants were infiltrated with distilled water and kept under normal photoperiod. Experiments were performed in triplicate; values are expressed as means  $\pm$  standard deviations (s.d.). Statistically significant differences ( $p \leq 0.05$ , ANOVA) are indicated by an asterisk.



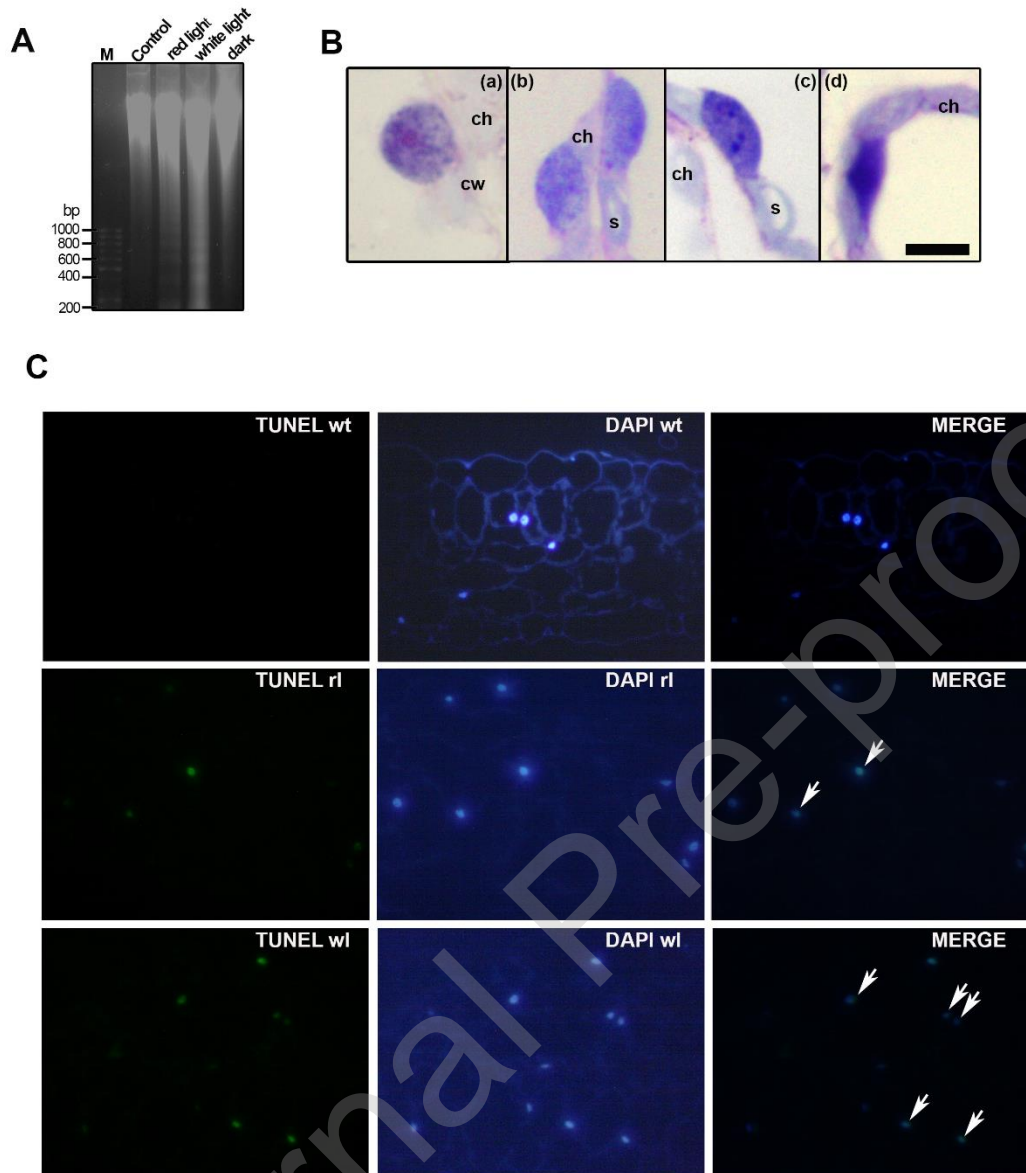
**Fig. 2.** RuBisCo levels in Pto DC3000-infiltrated tobacco leaves exposed to white light, red light, dark condition Control plants were infiltrated with distilled water and kept under normal photoperiod. For dark condition the leaves were covered with black cardboard envelopes. A polyclonal antiserum raised against the RuBisCo large subunit was used. (A)

*In situ* immunolocalization on semi-thin sections contrasted with toluidine blue O. **(B)** top: SDS-PAGE run; protein samples (10  $\mu$ L/lane) were separated on a 12 % polyacrylamide gel; bottom: RuBisCo was detected by Western Blot analysis. Scale bar: 50  $\mu$ m. Inset: 12.5  $\mu$ m. Abbreviations: ep, epidermis; n, nucleus; v, vacuole; me, mesophyll. Each image is a representative result of observation of at least five semi-thin sections.

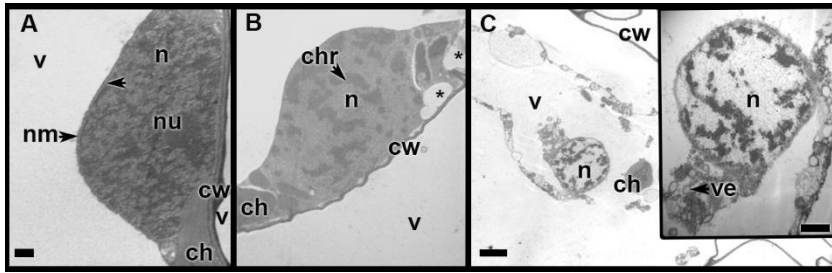


**Fig. 3.** DNA fragmentation analysis and nuclear disassembly **(A)** Genomic DNA fragmentation assay in leaves infiltrated with Pto DC3000 and exposed to white light, red light and dark condition. Control plants were infiltrated with distilled water and kept under normal photoperiod. For dark condition the leaves were covered with black cardboard

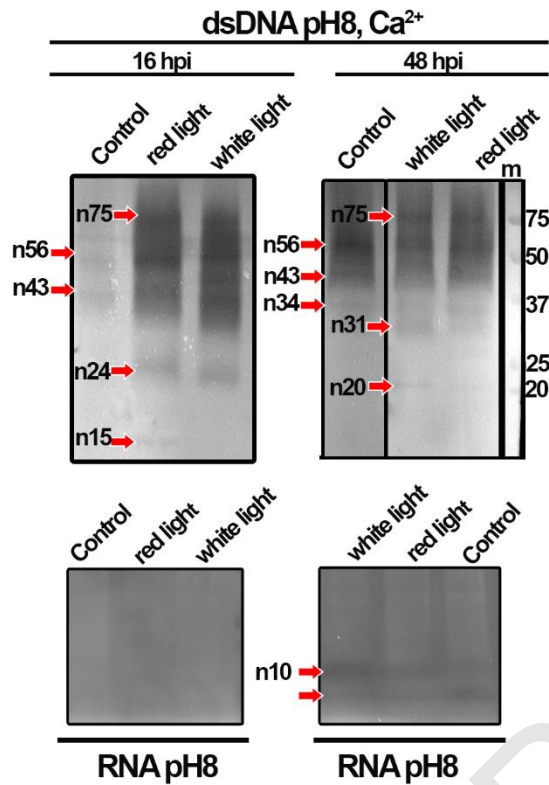
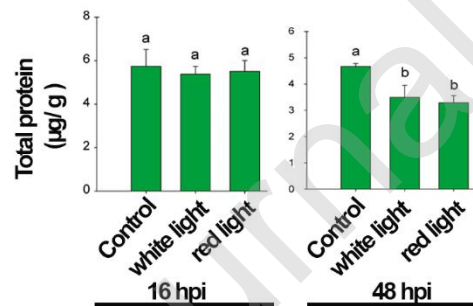
envelopes. Conventional agarose electrophoresis. Analyses were repeated at least three times on independent biological samples, and representative results are shown. **(B)** Progressive changes in nuclear morphology at 6 hpi (a) control (b) under red light, (c) and (d) under white light. Abbreviations: s, starch; cw, cell wall; ch, chloroplast. Scale bar= 5  $\mu\text{m}$ . **(C)** TUNEL assay (left column) and DAPI staining (central column) were performed on tissue sections of Pto DC3000-infiltrated leaves exposed to white and red light for 48 h. Control plants were infiltrated with distilled water and kept under normal photoperiod. Merged images (right column) confirmed that DAPI co-labeled TUNEL-positive nuclei. Scale bar= 50  $\mu\text{m}$ . Each image is a representative result of observation of at least six semi-thin sections of different infiltrated leaves.



**Fig. 4.** Progressive nuclei disassembly in *Pto* DC3000-infiltrated tobacco leaves exposed to white light at 16hpi (A) Control nucleus. (B-C) Nucleus affected during the HR process. \* indicate vacuoles. Abbreviations: ch, chloroplast; cw, cell wall; chr, chromatin; nm, nuclear membrane; nu, nucleoli; n, nucleus; v, vacuole; ve, vesicle. Scale bars: (A-B) 0.5  $\mu\text{m}$ ; (C) 2  $\mu\text{m}$ ; inset 0.2  $\mu\text{m}$ . In each case, the figure is a representative result of the observation of ultrathin sections from five different leaves at each stage, using TEM.



**Fig. 5.** (A) Determination of nuclease activity in Pto DC3000-infiltrated tobacco leaves exposed to white and red light for 16 and 48 h by using the *in-gel* activity assay with dsDNA or RNA as substrate. Control plants were infiltrated with distilled water and kept under normal photoperiod. The dsDNA gels were incubated in buffer pH 8 supplemented with  $\text{Ca}^{2+}$ , whereas the RNA gels were incubated in buffer pH 8 (B) Quantitative changes in total protein content for each light treatment. Each histogram is the mean  $\pm$  s.d. Analyses were repeated at least three times on independent biological samples, and representative results are shown. Different letters above the bars indicate significant differences between the corresponding data ( $p \leq 0.05$ , ANOVA).

**A****B**

**Fig. 6.** Immunoanalysis of Pto DC3000-infiltrated tobacco leaves exposed to white and red light using an anti-RcCys-EP antibody. Control plants were infiltrated with distilled water and kept under normal photoperiod. (A) Western Blot analysis with anti-RcCys-EP antibody

as primary antibody. Proteins (14  $\mu$ g) from Pto DC3000-infiltrated tobacco leaves exposed to different light treatments were separated on a 12 % polyacrylamide gel and then transferred to a nitrocellulose membrane. As a control, mock infiltrated leaves exposed to normal photoperiod and proteins (12  $\mu$ g) from 5-day germinating *Ricinus communis* seeds (R) were used. **(B)** A Coomassie stained SDS-PAGE was performed separately to ensure equal protein loading.

Journal Pre-proof

